Conference Applications of Mathematics 2013
in honor of the 70th birthday of Karel Segeth.
Jan Brandts, Sergey Korotov, Michal Křížek,
Jakub Šístek, and Tomáš Vejchodský (Eds.),
Institute of Mathematics AS CR, Prague 2013

HP-ANISOTROPIC MESH ADAPTATION TECHNIQUE BASED ON INTERPOLATION ERROR ESTIMATES

Vít Dolejší

Charles University Prague, Faculty of Mathematics and Physics
Sokolovská 83, 186 75, Prague, Czech Republic
dolejsi@karlin.mff.cuni.cz

Abstract

We present a completely new *hp*-anisotropic mesh adaptation technique for the numerical solution of partial differential equations with the aid of a discontinuous piecewise polynomial approximation. This approach generates general anisotropic triangular grids and the corresponding degrees of polynomial approximation based on the minimization of the interpolation error. We develop the theoretical background of this approach and present a numerical example demonstrating the efficiency of this anisotropic strategy in comparison with an isotropic one.

1. Introduction

Adaptive methods exhibit an efficient tool for the numerical solution of partial differential equations (PDEs). Our aim is to develop an adaptive technique which is able to generate general *hp*-anisotropic grids which can be employed in the framework of discontinuous Galerkin method based on a discontinuous piecewise polynomial approximation. The shape of an anisotropic element is extended in one dominant direction.

The *hp*-adaptive method allows the adaptation in the element size h as well as in the polynomial degree p. Several strategies of *hp*-adaptation have been proposed over the years, see, e.g., [14] or [11] for a survey. Based on many theoretical works, e.g., monographs [15] or papers [1, 5, 17] we expect that an error converges at an exponential rate in the number of degrees of freedom. However, most of *hp*-adaptive methods deal with h-isotropic refinement when the element marked for h-refinement is split (isotropically) into several (usually four in 2D) daughter elements. Some exception is, e.g., [13] where quadrilateral elements can be split onto two daughter elements by a line in a either vertical or horizontal direction.

Our goal is to generate anisotropic grids similarly to those ones developed, e.g., in [4, 6, 9, 12, 16], for the first order finite volume and finite element methods. In these works, the Hessian matrices (matrices of second order derivatives) are employed for the definition of a Riemann metric. Then the highly anisotropic triangular

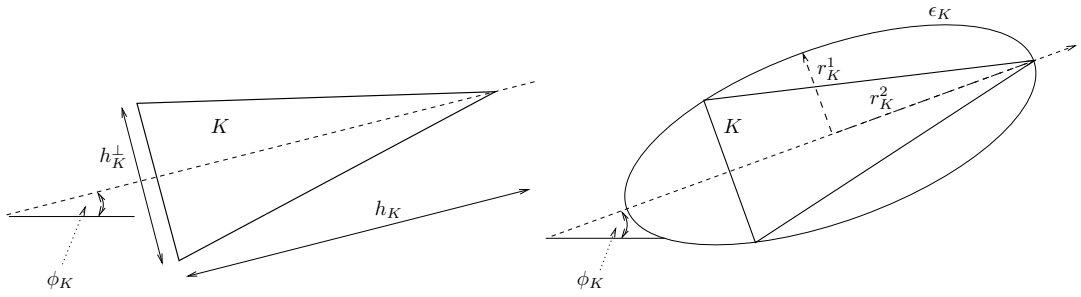

Figure 1: An anisotropic element K characterized by h_K, $h_K^\perp$ and ϕ_K (left), and an anisotropic element K characterized by r_K^1, r_K^2 and ϕ_K with the corresponding ellipse (right).

grids, which are quasi-uniform in this metric, are constructed. However, the Hessian matrices correspond to the interpolation error for a piecewise linear approximation. In [2, 3], the Riemann metric (defining the anisotropic mesh) is developed for a high degree of polynomial approximation. This approach is based on a particular definition of the magnitude, orientation, and anisotropic ratio for the higher order derivative of a function u to characterize its anisotropic behaviour. Being inspired by these papers, we develop here a new strategy which is able to generate anisotropic triangular grids and the corresponding degree of polynomial approximation for each element of the mesh. This approach is based on the approximation of the interpolation error in the L^∞-norm by the leading terms of the Taylor expansion. The aim is to keep the interpolation error under a given tolerance and to minimize the number of degree of freedom.

2. An anisotropic element

In this section, we describe an anisotropy of triangles in a plane domain. Let $K \subset \mathbb{R}^2$ be an acute isosceles triangle, see Figure 1, left. By h_K we denote its size in the direction of its axis, $h_K^\perp$ denotes its size in the direction perpendicular of its axis and $\phi_K \in [0, \pi)$ denotes the angle between its axis and the axis x_1, see Figure 1, left. The triple $(h_K, h_K^\perp, \phi_K)$ defines the *anisotropy* of element K.

We can define the anisotropy in an alternative way. Let $\lambda_K^1 > 0$, $\lambda_K^2 > 0$, and $\phi_K \in [0, \pi)$. We define the matrix M_K by

$$M_K := R^{\mathrm{T}}(\phi_K) \begin{pmatrix} \lambda_K^1 & 0 \\ 0 & \lambda_K^2 \end{pmatrix} R(\phi_K) = \begin{pmatrix} a_K & b_K \\ b_K & c_K \end{pmatrix}, \tag{1}$$

where $R(\phi_K)$ is the the rotation matrix

$$R(\phi_K) := \begin{pmatrix} \cos\phi_K & -\sin\phi_K \\ \sin\phi_K & \cos\phi_K \end{pmatrix} \tag{2}$$

and $R^{\mathrm{T}}(\phi_K)$ is its transpose matrix. Obviously, M_K is a symmetric positive definite matrix having eigenvalues λ_K^1, λ_K^2. The equation

$$x^{\mathrm{T}} M_K x = a_K x_1^2 + 2b_K x_1 x_2 + c_K x_2^2 \leq 1, \quad x = (x_1, x_2) \in \mathbb{R}^2, \tag{3}$$

defines an ellipse ϵ_K with the centre at origin, the semi-axes lengths

$$r_K^1 = 1/\sqrt{\lambda_K^1}, \quad r_K^2 = 1/\sqrt{\lambda_K^2} \tag{4}$$

and the angle between the axis x_1 and the major axis of ϵ_K is ϕ_K, see Figure 1, right.

Let K denotes an acute isosceles triangle which is inscribed into ellipse ϵ_K and which has the maximal possible area, see Figure 1, right. We say that K *is generated by* M_k. Hence, the anisotropy of this triangle K can be defined by the triple $(\lambda_K^1, \lambda_K^2, \phi_K)$ or the triple (r_K^1, r_K^2, ϕ_K). With the aid of techniques [7], we can derive direct relations between triples $(h_K, h_K^\perp, \phi_K)$ and $(\lambda_K^1, \lambda_K^2, \phi_K)$ (or (r_K^1, r_K^2, ϕ_K)). Namely, $h_K = \frac{3}{2} r_K^2$ and $h_K^\perp = 2\sqrt{3} r_K^1$.

Let $\boldsymbol{e}_i,\ i = 1, 2, 3$ denote the edges of the triangle K inscribed into ϵ_K and having the maximal area. The edges $\boldsymbol{e}_i,\ i = 1, 2, 3$ are considered as vectors from $\mathbb{R}^2$ given by their endpoints. In [6] we proved that

$$\|\boldsymbol{e}_i\|_{M_K} = \sqrt{3}, \quad i = 1, 2, 3, \tag{5}$$

where $\|\boldsymbol{e}_i\|_{M_K} := \left(\boldsymbol{e}_i^{\mathrm{T}} M_K \boldsymbol{e}_i\right)^{1/2}$ is the size of $\boldsymbol{e}_i$ in the Riemann metric generated by M_K, compare with Definition 3.1 bellow. Hence, K is the *equilateral triangle* in the *metric* generated by M_K.

3. *hp*-anisotropic meshes

Let the computational domain $\Omega \subset \mathbb{R}^2$ be bounded with a polygonal boundary $\partial\Omega$. Let $\mathscr{T}_h$ $(h > 0)$ be a partition of the closure $\overline{\Omega}$ of the domain Ω into a finite number of closed triangles K with mutually disjoint interiors. We call $\mathscr{T}_h = \{K\}_{K \in \mathscr{T}_h}$ a *triangulation* of Ω and assume that $\mathscr{T}_h$ is conforming.

Moreover, to each $K \in \mathscr{T}_h$, we assign a positive integer p_K (=local polynomial degree of polynomial approximation on K). Then we define the set $\mathbf{p} := \{p_K; K \in \mathscr{T}_h\}$ and the pair

$$\mathscr{T}_{h\mathbf{p}} := \{\mathscr{T}_h, \mathbf{p}\} \tag{6}$$

is called the *hp-mesh*.

For the given *hp*-mesh $\mathscr{T}_{h\mathbf{p}}$, we construct the space of piecewise polynomial discontinuous functions by

$$S_{h\mathbf{p}} = \{v \in L^2(\Omega);\ v|_K \in P^{p_K}(K)\ \forall K \in \mathscr{T}_h\}, \tag{7}$$

where $P^{p_K}(K)$ is the space of polynomials or degree $\leq p_K$ on $K \in \mathscr{T}_h$. The dimension of $S_{h\mathbf{p}}$ can be expressed (for two-dimensional domain) by

$$N_{h\mathbf{p}} := \sum_{K \in \mathscr{T}_h} (p_K + 1)(p_K + 2)/2. \tag{8}$$

We call this quantity the *size* of the *hp*-mesh $\mathscr{T}_{h\mathbf{p}}$.

Finally, by $\mathscr{F}_h$ we denote the set of edges of $\mathscr{T}_h$. Here the edges $\boldsymbol{e} \in \mathscr{F}_h$ are considered as vectors from $\mathbb{R}^2$ given by its endpoints. The orientation of the edges is arbitrary.

Similarly as in [4, 6, 9, 12, 16], we define the anisotropic triangular grid as a quasi-uniform grid in a Riemann metric.

Definition 3.1. *Let $\mathbf{M} : \Omega \to \mathbb{R}^{2\times 2}$ be a continuous mapping such that for each $x \in \Omega$, the matrix $\mathbf{M}(x)$ is symmetric and positive definite. Moreover, let $\boldsymbol{v}_0, \boldsymbol{v}_1 \in \mathbb{R}^2$ such that $\boldsymbol{v}_0 \in \Omega$ and $\boldsymbol{v}_0 + \boldsymbol{v}_1 \in \Omega$. The mapping $\boldsymbol{v} : [0,1] \to \mathbb{R}^2$, $\boldsymbol{v}(t) = \boldsymbol{v}_0 + t\boldsymbol{v}_1$, $t \in [0,1]$ defines a straight edge in Ω. Furthermore, we set*

$$\|\boldsymbol{v}\|_{\mathbf{M}} := \int_0^1 \left(\boldsymbol{v}'(t)^{\mathrm{T}}\mathbf{M}(\boldsymbol{v}_0 + t\boldsymbol{v}_1)\boldsymbol{v}'(t)\right)^{1/2} \mathrm{d}t = \int_0^1 \left(\boldsymbol{v}_1^{\mathrm{T}}\mathbf{M}(\boldsymbol{v}_0 + t\boldsymbol{v}_1)\boldsymbol{v}_1\right)^{1/2} \mathrm{d}t. \quad (9)$$

We call $\mathbf{M}$ the Riemann metric *on Ω and $\|\boldsymbol{v}\|_{\mathbf{M}}$ defines the* size *of edge $\boldsymbol{v}$ in the* Riemann metric $\mathbf{M}$.

Remark 3.2. *Let us note that if $\mathbf{M}$ is constant along $\boldsymbol{v}$ then* (9) *reduces to $\|\boldsymbol{v}\|_{\mathbf{M}} = (\boldsymbol{v}_1^{\mathrm{T}}\mathbf{M}\boldsymbol{v}_1)^{1/2}$. Moreover, if $\mathbf{M}(x) = \mathbb{I}\ \forall x \in \boldsymbol{v}$ ($\mathbb{I}$= the identity matrix) then the size of $\boldsymbol{v}$ in the Riemann metric $\mathbf{M}$ is equal to its length in the Euclidean metric.*

In virtue of (5), we define a triangulation corresponding to the metric $\mathbf{M}$.

Definition 3.3. *Let $\omega > 0$ be a given constant. Let $\mathbf{M}$ be the Riemann metric defined on Ω, $\mathscr{T}_h$ be a triangulation of Ω and $\mathscr{F}_h$ the corresponding set of edges. We say that the triangulation $\mathscr{T}_h$ is* generated by metric $\mathbf{M}$ *if*

$$\|\boldsymbol{e}\|_{\mathbf{M}} = \omega \quad \forall \boldsymbol{e} \in \mathscr{F}_h. \quad (10)$$

Remark 3.4. *For the given metric $\mathbf{M}$, there does not exist (except special cases) any triangulation generated by $\mathbf{M}$ in virtue of Definition 3.3. However, we can construct a triangulation which satisfies* (10) *approximately by the* least square technique*, see [6, 9]. Therefore, we replace* (10) *by $\|\boldsymbol{e}\|_{\mathbf{M}} \approx \omega\ \forall \boldsymbol{e} \in \mathscr{F}_h$ in the sense of the least square method. Moreover, let us note that for practical reasons, it is sufficient to evaluate the metric $\mathbf{M}$ only in a finite number of nodes $x \in \Omega$.*

Finally, let $\mathcal{P} : \Omega \to [0, \infty)$ be a given function. We define

$$p_K := \mathrm{int}\left[\frac{1}{|K|}\int_K \mathcal{P}(x)\,\mathrm{d}x\right], \quad K \in \mathscr{T}_h, \quad (11)$$

where $\mathrm{int}[a] := \lfloor a + 1/2 \rfloor$ denotes the integer part of the number $a + 1/2$, $a \geq 0$. We call $\mathcal{P}$ the *polynomial degree distribution function*.

We conclude that for the given Riemann metric $\mathbf{M}$ and for the given polynomial degree distribution function $\mathcal{P}$, there exists a *hp*-mesh $\mathscr{T}_{h\mathbf{p}} = \{\mathscr{T}_h, \mathbf{p}\}$, where $\mathscr{T}_h$ is given by Definition 3.3 in the sense of Remark 3.4 and $\mathbf{p}$ by (11). Our aim is to define the metric $\mathbf{M}$ and the polynomial degree distribution function $\mathcal{P}$ such that the corresponding *hp*-mesh is optimal in the sense specified later.

4. Interpolation error

For simplicity, we deal with the space of functions $V := C^\infty(\Omega)$. Let $\bar{x} = (x_1, x_2) \in \Omega$ be arbitrary but fixed. Let $p > 0$ be an integer, we define the interpolation operator $\Pi_{hp} : V \to P^p(\bar{\Omega})$ such that

$$\frac{\partial^k}{\partial x_1^l \partial x_2^{k-l}} \Pi_{hp} u(\bar{x}) = \frac{\partial^k}{\partial x_1^l \partial x_2^{k-l}} u(\bar{x}) \qquad \begin{matrix} \forall l = 0, \dots, k\,, \\ \forall k = 0, \dots, p\,. \end{matrix} \tag{12}$$

Therefore, $\Pi_{hp} u$ is the polynomial function of degree p on Ω which has the same value and the same values of all partial derivatives up to order p at $\bar{x}$ as the function u.

Using the Taylor expansion at $\bar{x} = (\bar{x}_1, \bar{x}_2)$, we have

$$u(x) = \sum_{k=0}^{p+1} \frac{1}{k!} \left(\sum_{l=0}^{k} \binom{k}{l} \frac{\partial^k u(\bar{x})}{\partial x_1^l \partial x_2^{k-l}} (x_1 - \bar{x}_1)^l (x_2 - \bar{x}_2)^{k-l} \right) + O(|x - \bar{x}|^{p+2}), \tag{13}$$

where $\binom{k}{l} = \frac{k!}{l\,!(k-l)!}$. From (12) and (13) we obtain

$$u(x) - \Pi_{hp} u(x) = E_{\mathrm{I}}^p(x) + O(|x - \bar{x}|^{p+2}), \tag{14}$$

where

$$E_{\mathrm{I}}^p(x) := \frac{1}{(p+1)!} \sum_{l=0}^{p+1} \left[\binom{p+1}{l} \frac{\partial^{p+1} u(\bar{x})}{\partial x_1^l \partial x_2^{p+1-l}} (x_1 - \bar{x}_1)^l (x_2 - \bar{x}_2)^{p+1-l} \right] \tag{15}$$

is the *interpolation error function* of degree $p = 0, 1, \dots$.

At this point, we consider the following task: Let $u \in V$, $\bar{x} \in \Omega$, $\omega > 0$ and $p > 0$ be given, we seek a triangle K' with barycentre at $\bar{x}$ such that

(C1) $E_{\mathrm{I}}^p(x) \le \omega$ for all $x \in K'$,

(C2) the area (two-dimensional Lebesgue measure) of K' is maximal.

The condition (C2) follows from the observation that a mesh having the maximal possible triangles has a small number of degree of freedom.

Let $B_1 := \{\xi;\ \xi = (\xi_1, \xi_2) \in \mathbb{R}^2,\ \xi_1^2 + \xi_2^2 = 1\}$ denote the unit sphere (in the Euclidean metric) in $\mathbb{R}^2$. We define the k^{th}-(scaled) *directional derivative* of $u \in V$ in $x \in \Omega$ and in the direction ξ by

$$\mathrm{d}^k u(x; \xi) := \frac{1}{k!} \sum_{l=0}^{k} \binom{k}{l} \frac{\partial^k u(x)}{\partial x_1^l \partial x_2^{k-l}} \xi_1^l \xi_2^{k-l}, \quad x \in \Omega,\ \xi = (\xi_1, \xi_2) \in B_1. \tag{16}$$

Therefore, from (15) and (16), we have

$$E_{\mathrm{I}}^p(x) = \mathrm{d}^{p+1} u \left(\bar{x}; \frac{x - \bar{x}}{|x - \bar{x}|} \right) |x - \bar{x}|^{p+1}, \quad p = 0, 1, \dots,\ x \in \Omega. \tag{17}$$

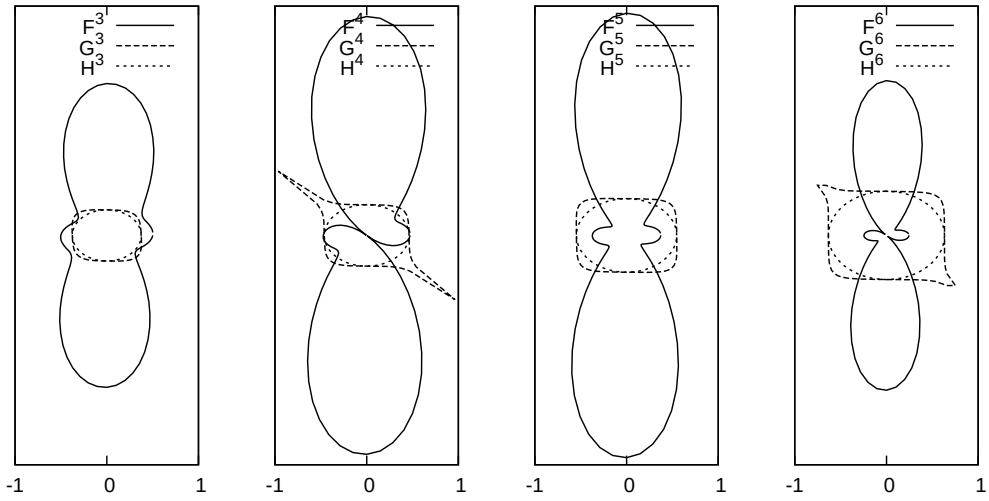

Figure 2: The curve F^p, the domain G^p and the ellipse H^p for $p = 3, 4, 5, 6$, $\bar{x} = (0, 0)$ and the function u given by (20).

Let $u \in V$, $\bar{x} \in \Omega$, $\omega > 0$ and $p > 0$ be given. We define the sets

$$F^p := \left\{ x \in \mathbb{R}^2;\ x = \bar{x} + \xi \left| \mathrm{d}^{p+1} u(\bar{x}; \xi) \right|,\ \xi \in B_1 \right\}, \tag{18}$$

$$G^p := \left\{ x \in \mathbb{R}^2;\ x = \bar{x} + t\xi \left(\frac{\omega}{|\mathrm{d}^{p+1} u(\bar{x}; \xi)|} \right)^{\frac{1}{p+1}},\ t \in [0; 1],\ \xi \in B_1 \right\}, \tag{19}$$

where $p = 1, 2, \ldots$. If $x \in F^p$ then the directional derivative $\mathrm{d}^{p+1} u(\bar{x}, \cdot)$ in the direction $(x - \bar{x})/|x - \bar{x}|$ is equal to $|x - \bar{x}|$. Moreover, in virtue of (17) and (19), G^p is the set such that $E^p_{\mathrm{I}}(x) \leq \omega\ \forall x \in G^p$. The set F^p is one-dimensional continuous curve in $\mathbb{R}^2$ whereas G^p is two dimensional sub-domain of $\mathbb{R}^2$ (it may be unbounded if $\mathrm{d}^{p+1} u(\bar{x}; \xi) = 0$ for some ξ). Figure 2 shows the curve F^p and the domain G^p for $p = 3, 4, 5, 6$, $\bar{x} = (0, 0)$ and the function

$$u(x_1, x_2) = 10x_1^{10} + 2x_1^{10}x_2^6 + x_1^9 x_2 + 2x_1^8 x_2^3 - x_1^7 x_2^5 + 8x_1^4 x_2^6 + 2x_2^{10}. \tag{20}$$

From (19) we find that if K is a triangle with the barycentre $\bar{x}$ such that $K \subset G^p$ for some p then $E^p_{\mathrm{I}}(x) \leq \omega$ for all $x \in K$. In order to minimize the number of degree of freedom of $S_{h_{\mathbf{p}}}$, the aim is to have triangle K such that $K \subset G^p$ and K has the maximal possible area.

5. Definition of the metric

In the following, with the aid of the results from Section 4, we define the Riemann metric $\mathbf{M}$ and the polynomial degree distribution function $\mathcal{P}$ introduced in Section 3.

Let $\bar{x} \in \Omega$, $u \in V$ and $p \geq 1$. Let $\xi_p^{\max} \in B_1$ be the direction which maximizes $|\mathrm{d}^p u(\bar{x};\xi)|$ and $\xi_p^{\perp}$ the direction orthogonal, i.e,

$$\xi_p^{\max} := \arg\max_{\xi \in B_1} |\mathrm{d}^p u(\bar{x};\xi)|, \quad \xi_p^{\perp} \in B_1, \quad \xi_p^{\max} \cdot \xi_p^{\perp} = 0. \tag{21}$$

Then we define quantities

$$h_p^{\max} := \left(\frac{\omega}{\left|\mathrm{d}^{p+1} u(\bar{x};\xi_p^{\max})\right|} \right)^{1/(p+1)}, \quad h_p^{\min} := \left(\frac{\omega}{\left|\mathrm{d}^{p+1} u(\bar{x};\xi_p^{\perp})\right|} \right)^{1/(p+1)}. \tag{22}$$

Let us note that $h_p^{\max} \leq h_p^{\min}$. Moreover, let $\phi_p \in [0, 2\pi)$ be such that $\xi_p^{\max} = (\cos\phi_p, \sin\phi_p) \in B_1$. Hence, the triple

$$\{h_p^{\min}, h_p^{\max}, \phi_p\} \tag{23}$$

defines the ellipse H^p which touches G^p at the nearest point to $\bar{x}$, see Figure 2. Moreover, we have observed experimentally that H^p is almost included in G^p.

Therefore, in virtue of (1), (4) and Definition 3.1, we define the metric $\mathbf{M}$ at $\bar{x}$ by $\mathbf{M}(\bar{x}) := M_p$, where

$$M_p := R^{\mathrm{T}}(\phi_p) \begin{pmatrix} 1/(h_p^{\max})^2 & 0 \\ 0 & 1/(h_p^{\min})^2 \end{pmatrix} R(\phi_p), \quad K \in \mathscr{T}_h,\ p \geq 1, \tag{24}$$

and $R(\phi_p)$ is given by (2).

Finally, we have to define the polynomial degree distribution function $\mathcal{P}(x)$ at $\bar{x} \in \Omega$. For each integer $p \geq 1$ we have matrix $\mathbf{M}(\bar{x}) := M_p$. We seek some criterion choosing giving the optimal degree of polynomial approximation p. The aim is to minimize $N_{h\mathbf{p}}$ (=size of the hp-mesh). The area of the element K generated by M_p is proportional to the area of the ellipse defined by relation $\xi^{\mathrm{T}} M_p \xi = 1$, $\xi \in B_1$, namely $|K| = (2\sqrt{3}/2) h_p^{\max} h_p^{\min}$. If $|K|$ is an average volume of triangles from $\mathscr{T}_h$ then we need approximately $\lfloor |\Omega|/|K| \rfloor$ triangles. If p is the degree of polynomial approximation, the total number of freedom for one element is $(p+1)(p+2)/2$ and the value $N_{h\mathbf{p}}$ can be estimated (up to a constant)

$$N_{h\mathbf{p}} \approx \frac{(p+1)(p+2)}{2} \frac{|\Omega|}{|K|}. \tag{25}$$

Then we deduce that in order to minimize $N_{h\mathbf{p}}$, we need to choose the degree of polynomial approximation p such that

$$\mathcal{P}(\bar{x}) = \arg\min_{p=1,2,\ldots} \frac{(p+1)(p+2)}{h_p^{\max} h_p^{\min}}. \tag{26}$$

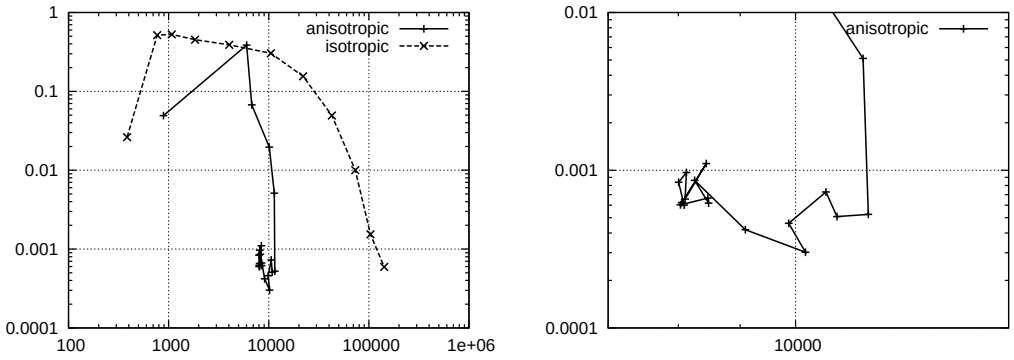

Figure 3: Comparison of the isotropic and the anisotropic *hp*-adaptation, the dependence of the error in the X-norm with respect to the degree of freedom $N_{h\mathbf{p}}$, the total view (left) and the detail (right).

6. Numerical implementation

In Sections 2–5, we developed the method which defines the metric $\mathbf{M}(x)$ and the polynomial degree distribution function $\mathcal{P}(x)$ for $x \in \Omega$. Hence, in virtue of the conclusion of Section 3, we have defined the *hp*-mesh for a given function $u \in V_h$.

The aim is to employ this strategy for the numerical solution of partial differential equations. Since the exact solution u is unknown, the natural approach is to apply the previous *hp*-anisotropic mesh adaptation method to some smoothing of the approximate solution $u_{h\mathbf{p}} \in S_{h\mathbf{p}}$. We obtain iteratively better and better *hp*-grids and the corresponding approximate solutions. Moreover, for practical computation, it is not necessary to evaluate $\mathbf{M}(x)$ and $\mathcal{P}(x)$ for all $x \in \Omega$. It is enough to compute $\mathbf{M}(x_K)$ and $\mathcal{P}(x_K)$ for all elements K of the given mesh (x_K is the barycentre of K), similarly as in [6, 9].

We demonstrate the potential of the proposed *hp*-anisotropic mesh adaptation method by a comparison with the isotropic *hp*-adaptation method presented in [8]. We consider the scalar linear convection-diffusion equation (similarly as in [10])

$$-\varepsilon\triangle u - \frac{\partial u}{\partial x_1} - \frac{\partial u}{\partial x_2} = g \quad \text{in } \Omega := (0,1)^2, \tag{27}$$

where $\varepsilon > 0$ is a constant diffusion coefficient. We prescribe a Dirichlet boundary condition on $\partial\Omega$ and the source term g such that the exact solution has the form $u(x_1, x_2) = \left(c_1 + c_2(1-x_1) + \mathrm{e}^{-x_1/\varepsilon}\right)\left(c_1 + c_2(1-x_2) + \mathrm{e}^{-x_2/\varepsilon}\right)$ with $c_1 = -\mathrm{e}^{-1/\varepsilon}$, $c_2 = -1 - c_1$. The solution contains two boundary layers along $x_1 = 0$ and $x_2 = 0$, whose width is proportional to ε. Here we consider $\varepsilon = 10^{-3}$.

We solve (27) with the aid of discontinuous Galerkin method with an interior penalty. Figure 3 shows the convergence of the computational error in the norm $\|\cdot\|_X^2 := \|\cdot\|_{L^2(\Omega)}^2 + \varepsilon|\cdot|_{H^1(\Omega)}^2$ with respect to the number of degree of freedom. We observe that the *hp*-anisotropic mesh adaptation is more efficient. Moreover, the

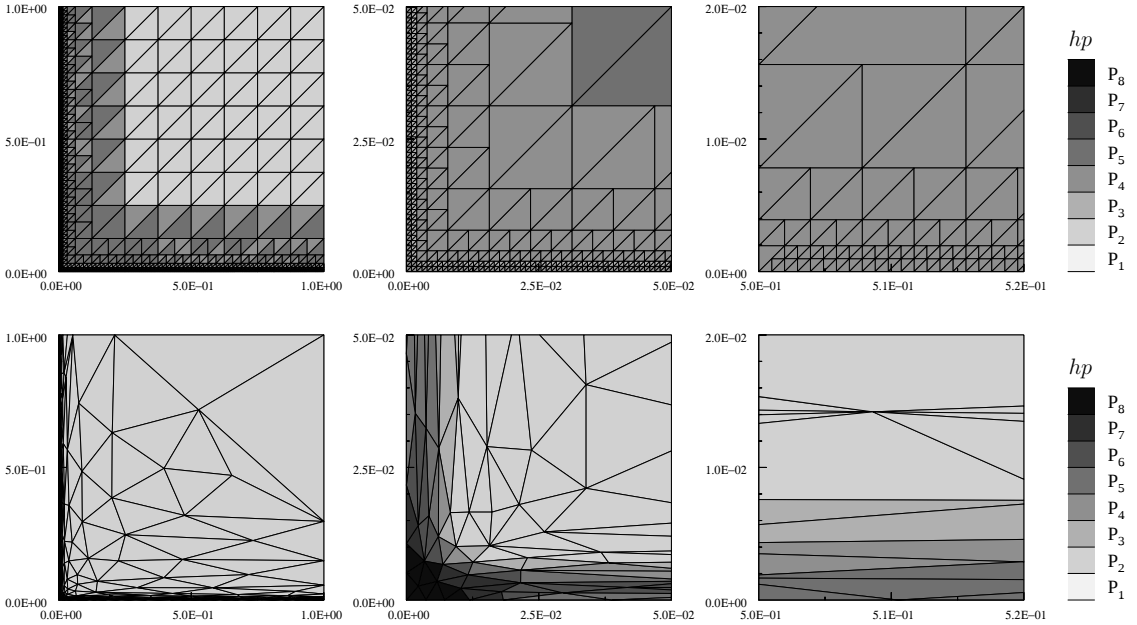

Figure 4: Example (E1): the final *hp*-meshes obtained be the isotropic (top) and the anisotropic (bottom) *hp*-adaptation, the total view (left), the detail around the corner (centre) and the detail of the boundary layer (right).

proposed technique is able to reduce the number of degree of freedom and to keep the level of the computational error during the optimization of the *hp*-mesh. Figure 4 shows the final grids obtained by the isotropic and the anisotropic technique.

Acknowledgements

This work was supported by grant No. 13-00522S of the Czech Science Foundation.

References

[1] Babuška, I. and Suri, M.: The $p-$ and $hp-$FEM a survey. SIAM Review **36** (1994), 578–632.

[2] Cao, W.: Anisotropic measures of third order derivatives and the quadratic interpolation error on triangular elements. SIAM J. Sci. Comput. **29** (2007), 756–781.

[3] Cao, W.: An interpolation error estimate in R^2 based on the anisotropic measures of higher order derivatives. Math. Comp. **77** (2008), 265–286.

[4] Castro-Díaz, M. J., Borouchaki, H., George, P. L., Hecht, F., and Mohammadi, B.: Anisotropic Adaptive Mesch Generation in Two Dimensions for CFD. In: J.A. Désidéri, C. Hirsch, P. Le Tallec, M. Pandolfi, and J. Périaux (Eds.), *Computational Fluid Dynamics '96*. Wiley, Chichester, Paris, 1996 pp. 181–186.

[5] Demkowicz, L., Rachowicz, W., and Devloo, P.: A fully automatic *hp*-adaptivity. J. Sci. Comput. **17** (2002), 117–142.

[6] Dolejší, V.: Anisotropic mesh adaptation for finite volume and finite element methods on triangular meshes. Comput. Vis. Sci. **1** (1998), 165–178.

[7] Dolejší, V.: *Adaptive higher order methods for compressible flow*, chap. Anisotropic mesh adaptation method. Charles University Prague, Faculty of Mathematics and Physics, 2003. Habilitation thesis.

[8] Dolejší, V.: *hp*-DGFEM for nonlinear convection-diffusion problems. Math. Comput. Simul. (submitted). Preprint No. MATH-knm-2012/2, Charles University Prague, www.karlin.mff.cuni.cz/ms-preprints.

[9] Dolejší, V. and Felcman, J.: Anisotropic mesh adaptation and its application for scalar diffusion equations. Numer. Methods Partial Differential Equations **20** (2004), 576–608.

[10] Dolejší, V. and Roos, H. G.: BDF-FEM for parabolic singularly perturbed problems with exponential layers on layer-adapted meshes in space. Neural Parallel Sci. Comput. **18** (2010), 221–235.

[11] Eibner, T. and Melenk, J. M.: An adaptive strategy for *hp*-FEM based on testing for analyticity. Comput. Mech. **39** (2007), 575–595.

[12] Fortin, M., Vallet, M. G., Dompierre, J., Bourgault, Y., and Habashi, W. G.: Anisotropic Mesh Adaptation: Theory, Validation and Applications. In: J. A. Désidéri, C. Hirsch, P. Le Tallec, M. Pandolfi, and J. Périaux (Eds.), *Computational Fluid Dynamics '96*. Wiley, Chichester, Paris, 1996 pp. 174–180.

[13] Giani, S. and Houston, P.: Anisotropic *hp*-adaptive discontinuous Galerkin finite element methods for compressible fluid flows. International Journal of Numerical Analysis and Modeling **9** (2012), 928–949.

[14] Houston, P. and Süli, E.: A note on the design of *hp*–adaptive finite element methods for elliptic partial differential equations. Comput. Methods Appl. Mech. Engrg. **194** (2005), 229–243.

[15] Schwab, C.: *p- and hp-Finite Element Methods*. Clarendon Press, Oxford, 1998.

[16] Simpson, R. B.: Anisotropic mesh transformations and optimal error control. Appl. Numer. Math. **14** (1994), 183–198.

[17] Šolín, P. and Demkowicz, L.: Goal-oriented *hp*-adaptivity for elliptic problems. Comput. Methods Appl. Mech. Engrg. **193** (2004), 449–468.